PHYSICAL REVIEW B VOLUME 10, NUMBER 3 1 AUGUST 1974

Properties of the Hubbard Hamiltonian including the resonance-broadening terms for an arbitrarily filled band

L. C. Bartel*
Sandia Laboratories, Albuquerque, New Mexico 87115

H. S. Jarrett
E. I. du Pont de Nemours and Company, Wilmington, Delaware 19898

(Received 12 December 1973)

In this paper, resonance broadening is included along with spin-disorder scattering to study the properties of the Hubbard Hamiltonian. Our solution, obtained through use of the locator technique, is valid for all strengths of the Coulomb repulsion term and for all band occupancies. However, here we restrict our work to the strong-correlation limit. We find that inclusion of the resonance-broadening terms (in particular spin-flip scattering) leads to qualitative differences in the pseudoparticle density of states compared with the density of states obtained with spin-disorder scattering only. When all three of Hubbard's scattering terms are included, the ground state is nonferromagnetic for any level of band filling. We also calculate the specific heat, magnetic susceptibility, and spin-spin correlation function as a function of temperature. Partial band occupancy yields a Pauli-like susceptibility at low temperature that transforms smoothly to Curie-like behavior at high temperature. The specific heat exhibits one or two maxima depending on occupancy, but these maxima are not reflected in the susceptibility and seem to be associated, not with magnetic ordering transitions, but with excitations across the Mott-Hubbard gap.

I. INTRODUCTION

Over the years considerable attention has been given to possible solutions to the Hubbard model Hamiltonian.[1] It is beyond the scope of this paper to review all methods; however, in a recent paper, Esterling and Dubin[2] reviewed some of these solutions and discussed their moment-generated solution. These previous solutions include exact results in one dimension, as well as, Green's-function, perturbation, path-formulation, variational, and functional integral techniques. Recently, a theory for disordered alloys, the coherent-potential approximation (CPA),[3,4] has been used to investigate the magnetic properties of the Hubbard model Hamiltonian in the strong-correlation limit; e.g., see papers by Levin and Bennemann[5] and Fukuyama and Ehrenreich.[6]

In Hubbards's solution,[1] the common approximation of truncating the Green's-function equations of motion is made in the second-order equation. Even this simplification leads to exceedingly complicated mathematics, and subsequent investigators during the past ten years have resorted to additional approximations, e.g., series expansion in the strong- or weak-correlation limit, high-temperature expansion, CPA single-scattering approximation, and weak applied fields. These approximations are valid only in extreme limits and do not express the behavior of Hubbard's solution over the entire range of variables. Hubbard himself simplified the mathematics by assuming a half-filled nonmagnetic band with a circular density of states and zero temperature. In this paper, we carry through the complete Hubbard solution by computer methods for all correlation energies, temperatures, and band occupancy, assuming only that the single-particle density of states is circular.

In Hubbard's alloy analogy,[1] which has been shown to be equivalent to the CPA[4] for a single scattering mechanism, the position of the $-\sigma$ spin electron is held fixed while the motion of the σ spin electron is watched. The relevant scattering term in the CPA is spin-disorder scattering and is analogous to potential scattering in an alloy. As pointed out by Hubbard,[1] the analogy would be exact if by some means the positions of the $-\sigma$ spin electrons remain fixed while the σ spin electron hops from site to site. The motion of the $-\sigma$ electron is taken into account by including what Hubbard called the resonance-broadening terms. These resonance-broadening terms are the scattering of a σ spin electron into a $-\sigma$ spin hole and the spin-flip scattering, in which an atom absorbs a σ spin electron and emits a $-\sigma$ spin electron, thus coupling the motion of σ and $-\sigma$ spin particles. These resonance-broadening terms have largely been ignored in favor of the computationally simpler CPA.

Recently, Jarrett[7] investigated the effects of Hubbard's three scattering terms on the ferromagnetic bandwidths for a half-filled band. He discovered the inclusion of the spin-flip scattering term has a significant effect on the density of states. In particular, the bandwidths for the σ

and $-\sigma$ spin bands remain the same for any magnetization when all three scattering terms are included, in sharp contrast to results when only the spin-disorder CPA and/or the σ-spin-electron into a $-\sigma$-spin-hole scattering terms are included.

In a separate publication,[8] we have calculated the possible ferromagnetic states for a partially filled band at $T=0$ only with all three scattering terms and have compared the results to CPA calculations. In that publication we assumed a symmetry in the interactor, which is strictly true only for the half-filled band. However, as we shall discuss, we find that for an arbitrarily filled band the symmetry relation is approximately obeyed. We conclude from our previous work,[7,8] and from the work in this paper, that in the strong-correlation limit, solutions (CPA, variational, moment-generated, perturbation, etc.) which might exclude spin-flip scattering lead to qualitatively different results than those where it is included.

Shiba and Pincus[9] studied the thermodynamic properties of the one-dimensional half-filled-band Hubbard model using the approach of Bonner and Fisher. They also compared their numerical results for the one-dimensional case to results obtained using what they term Hubbard's "improved" approximate theory.[1] (Hubbard's "improved" approximate theory is identical to the inclusion of the three scattering terms discussed above.) They found that Hubbard's theory[1] semiquantitatively reproduced their results for finite chains for the thermal properties in the high-temperature region, if the Coulomb repulsion term was large compared to the bandwidth. They also found that spin-wave contributions, which are neglected in Hubbard's theory,[1] are important for the low-temperature behavior of the specific heat as well as susceptibility.[9]

Out of all the possible scattering terms, the three scattering terms discussed above arise from the particular truncation scheme of the Green's functions employed by Hubbard. This scheme is identical to the locator technique,[10,11] in which it is assumed that the scattering rate for an average atom at the origin in a lattice of average atoms is equal to the configurational average of the scattering by the various component atoms replacing the average atom at the origin. We employ locator formalism for an arbitrarily filled band, for all values of the Coulomb repulsive energy and finite temperature.

Our solution contains no approximation beyond those contained in the locator technique, no high-temperature expansion, and no expansion in the ratio of bandwidth to Coulomb repulsive energy. In spite of the general validity of this solution, we restrict our discussions in this paper to the strong-correlation limit and defer discussion of the weak-correlation limit to a future publication.

In Sec. II, we develop the locator technique. The ground state, density of states, electronic specific heat, and magnetic susceptibility, all in the strong-correlation limit, are discussed in Sec. III. Finally, in Sec. IV we summarize our findings and give our conclusions.

II. SOLUTION TO THE HUBBARD HAMILTONIAN

The Hubbard model Hamiltonian[1] is given by

$$\mathcal{H}=\sum_{ij\sigma} t_{ij}C_{i\sigma}^{\dagger}C_{j\sigma}+\sum_{i\sigma} T_0 n_{i\sigma}+I\sum_i n_{i\uparrow}n_{i\downarrow}\,, \quad (1)$$

where t_{ij} is the hopping matrix element for an electron hopping from site j to site i, with $t_{ii}=0$. T_0 is the atomic binding energy, the C's are the electron operators with $n_{i\sigma}=C_{i\sigma}^{\dagger}C_{i\sigma}$, and I is the Coulomb repulsion energy for electrons of opposite spin localized on the same site. In the atomic limit for either a σ or a $-\sigma$ spin electron on an otherwise empty site, the electron has an energy T_0; for a σ and $-\sigma$ spin electron on the same site, the energy is T_0+I. More than one electron of the same spin is forbidden to occupy a site, because of the exclusion principle. For finite t_{ij} these atomic states broaden into the so-called Hubbard bands, one centered at T_0 and the other at T_0+I, separated by the Mott-Hubbard gap of width approximately $I-\Delta$, where Δ is the bandwidth. For a circular single-particle density of states and $I/\Delta>\frac{1}{2}\sqrt{3}$ with occupancy $n=1$, there exist two distinct bands.[1] For $I/\Delta<\frac{1}{2}\sqrt{3}$ with $n=1$, the bands merge into a single band. In the limit of $I/\Delta\ll\frac{1}{2}\sqrt{3}$, the motions of the electrons become quite rapid, such that a motional narrowing takes place, and a σ spin electron "sees" the average energy $In_{-\sigma}$.[1] This probably corresponds to the Hartree-Fock (HF) limit. However, Bari and Kaplan[12] point out that, in the absence of electron scattering (Hubbard I), the weak-correlation limit is not the HF limit.

The self-consistency relation in locator formalism becomes

$$\frac{1}{E-\Sigma^{0}(E)-\Omega_{\sigma}(E)}=\frac{x}{E-E_A-\Omega_{\sigma}(E)}+\frac{y}{E-E_B-\Omega_{\sigma}(E)}\,, \quad (2)$$

where the right-hand side (r.h.s) is the configurational-average Green's function, and the left-hand side (l.h.s.) is the Green's function for the lattice of average atoms. Here E is the energy and for a half-filled band $x+y=1$; $\Sigma^{0}(E)$ is the self-energy for the σ spin electron; $\Omega_{\sigma}(E)$ is the renormalized

interactor[1,10,11] for the σ spin electron; and E_A and E_B are the atomic energies for the A and B atoms, respectively. $\Omega_\sigma(E)$ (designated U_0 by Blackman *et al.*[11]) represents the kinetic energy of an electron dressed by multiparticle scattering hopping between atomic sites. In the magnetic case discussed here, $E_A=-E_B=\frac{1}{2}I$. This assignment places the origin of E (which is taken at the atomic binding energy T_0 in the Hubbard model) at $-\frac{1}{2}I$. The concentrations x and y become the fractional number of down n_- and up n_+ electrons, as discussed below.

For less than one electron per site ($n<1$), there are some empty sites, and a σ spin electron can hop from a site with only the σ spin electron on it to the previously empty site, with no change in energy (the case is similar for a $-\sigma$ spin electron). In discussing the motion of the σ spin electron, the r.h.s. of Eq. (2) becomes $x[E-E_A-\Omega_\sigma(E)]^{-1}+y[E-E_B-\Omega_\sigma(E)]^{-1}+z[E-E_C-\Omega_\sigma(E)]^{-1}$, where now $x+y+z=1$, $x=n_{-\sigma}$, $y=n_\sigma$, $z=1-n$, $n_\sigma+n_{-\sigma}=n$, $E_A=\frac{1}{2}I$, and $E_B=E_C=-\frac{1}{2}I$. The expression corresponding to Eq. (2) now becomes

$$\frac{1}{E-\Sigma^\sigma(E)-\Omega_\sigma(E)}=\frac{n_{-\sigma}}{E-\frac{1}{2}I-\Omega_\sigma(E)}+\frac{1-n_{-\sigma}}{E+\frac{1}{2}I-\Omega_\sigma(E)}, \tag{3}$$

which is the self-consistency relation that we shall use in our following work. Note that solving Eq. (3) for $[E-\Sigma^\sigma(E)]^{-1}$ gives Hubbard's[1] Eq. (59), where Hubbard's $F^\sigma(E)=[E-\Sigma^\sigma(E)]$, see Ref. 4.

From the definition of the interactor $\Omega_\sigma(E)$ [Blackman *et al.*[11] Eq. (2.7), or Shiba[10] Eq. (2.13)]

$$\frac{1}{E-\Sigma^\sigma(E)-\Omega_\sigma'(E)}=\frac{1}{N}\sum_{\vec{k}}\frac{1}{E-\Sigma^\sigma(E)-\epsilon_{\vec{k}}}\equiv G_{00}^\sigma(E), \tag{4}$$

where $\Omega_\sigma'(E)$ is to be distinguished from $\Omega_\sigma(E)$. In the ordinary CPA there is only the spin-disorder scattering and $\Omega_\sigma'(E)=\Omega_\sigma(E)$, and the resulting self-consistency relation from Eq. (3) is just the usual CPA self-consistency relation of Soven[3] and of Velický *et al.*[4] However, in Hubbard III, Ref. 1, there are three scattering mechanisms. The first, spin-disorder scattering, is analogous to potential scattering in an alloy. The other two, designated "resonance broadening," include scattering of a σ spin electron into a $-\sigma$ spin hole and spin-flip scattering. The total interactor is taken to be the sum of the interactors of the above three scattering processes[1]

$$\Omega_\sigma(E)=\Omega_\sigma'(E)-\Omega_{-\sigma}'(-E)+\Omega_{-\sigma}'(E). \tag{5}$$

Equation (5) represents four simultaneous equations in $\pm\sigma$ and $\pm E$. From Eq. (4) we have, for $\Omega_\sigma'(E)$,

$$\Omega_\sigma'(E)=E-\Sigma^\sigma(E)-[G_{00}^\sigma(E)]^{-1}. \tag{6}$$

To facilitate the calculations, it is desirable to obtain an analytical expression between $\Sigma^\sigma(E)$ and $G_{00}^\sigma(E)$. Such an expression exists when the single-particle density of states of bandwidth Δ is given by

$$\rho^{(0)}(E)=\begin{cases}(8/\pi\Delta^2)[(\frac{1}{2}\Delta)^2-E^2]^{1/2}, & |E|\leq\frac{1}{2}\Delta\\ 0, & |E|>\frac{1}{2}\Delta\end{cases}. \tag{7}$$

From Eq. (4), $G_{00}^\sigma(E)$ becomes

$$G_{00}^\sigma(E)=\int_{-\infty}^{\infty}\frac{\rho^{(0)}(\epsilon)\,d\epsilon}{E-\Sigma^\sigma(E)-\epsilon}, \tag{8}$$

yielding the result

$$\Sigma^\sigma(z)=z-[G_{00}^\sigma(z)]^{-1}-\tfrac{1}{4}G_{00}^\sigma(z),\quad z=E+i0, \tag{9}$$

where the energy is now expressed in units of half-band-widths.[4] From Eqs. (6) and (9), we obtain

$$\Omega_\sigma(E)=\tfrac{1}{4}[G_{00}^\sigma(E)-G_{00}^{-\sigma}(-E)+G_{00}^{-\sigma}(E)]. \tag{10}$$

For the half-filled band, there is a particle-hole symmetry such that $\Omega_\sigma(E)=-\Omega_{-\sigma}(-E)$. For a less-than half-filled band, this relationship for $\Omega_\sigma(E)$ is not strictly obeyed. However, by actual calculation of various properties, the error in assuming $\Omega_\sigma(E)=-\Omega_{-\sigma}(-E)$ for all band occupancy is 5% or less when compared with the calculations, which follow, and where particle-hole symmetry is not assumed.

By solving Eq. (3) for $\Omega_\sigma(E)$ and using Eq. (10), we have, for $g_\sigma^+[\equiv G_{00}^\sigma(E)]$ and $g_\sigma^-[\equiv G_{00}^\sigma(-E)]$,

$$\begin{aligned}-\tfrac{1}{16}(g_\sigma^+)^3+\tfrac{1}{2}E(g_\sigma^+)^2+[(\tfrac{1}{2}I)^2-E^2-\tfrac{1}{4}]g_\sigma^+ +E-\Gamma_{-\sigma}\\ +\tfrac{1}{16}(g_\sigma^+)^2g_{-\sigma}^- -\tfrac{1}{4}(E+\Gamma_{-\sigma})g_\sigma^+g_{-\sigma}^- +\tfrac{1}{4}g_{-\sigma}^-\\ -\tfrac{1}{16}(g_\sigma^+)^2g_{-\sigma}^+ +\tfrac{1}{4}(E+\Gamma_{-\sigma})g_\sigma^+g_{-\sigma}^+ -\tfrac{1}{4}g_{-\sigma}^+=0,\end{aligned} \tag{11}$$

where

$$\Gamma_\sigma=\tfrac{1}{2}I(1-2n_\sigma). \tag{12}$$

Equation (11) represents four simultaneous equations in $\pm\sigma$ and $\pm E$ to be solved for $g_{\pm\sigma}^\pm$.

In the paramagnetic regime, $G_{00}^\sigma(E)=G_{00}^{-\sigma}(E)$ ($g_\sigma^+=g_{-\sigma}^+$) and then Eq. (11) becomes

$$\begin{aligned}-\tfrac{1}{8}(g_\sigma^+)^3+(\tfrac{3}{4}E+\tfrac{1}{4}\Gamma_{-\sigma})(g_\sigma^+)^2+[(\tfrac{1}{2}I)^2-E^2-\tfrac{1}{2}]g_\sigma^+\\ +E-\Gamma_{-\sigma}+\tfrac{1}{16}(g_\sigma^+)^2g_{-\sigma}^-\\ -\tfrac{1}{4}(E+\Gamma_{-\sigma})g_\sigma^-g_{-\sigma}^+ +\tfrac{1}{4}g_{-\sigma}^-=0.\end{aligned} \tag{13}$$

Equation (13) represents two simultaneous equations to be solved for g_σ^+ and $g_{-\sigma}^-$. By eliminating g_-^- in Eq. (13), for example, the resulting poly-

nomial in g_+^+ is ninth order; this is displayed in Appendix A.

The pseudoparticle density of states is given by

$$\rho_\sigma(E) = -\pi^{-1}\,\mathrm{Im}G_{00}^{\sigma}(E), \tag{14}$$

and n_σ is given by

$$n_\sigma = -\pi^{-1}\int_{-\infty}^{\infty} dE\, f(E)\,\mathrm{Im}G_{00}^{\sigma}(E), \tag{15}$$

where $f(E)$ is the Fermi distribution function, $n = n_+ + n_-$, and $m = n_+ - n_-$; n is the average number of electrons per site and m is the average magnetization per site. The total electronic internal energy is calculated following Kjöllerstrom *et al.*[13] to be

$$E_T = -\pi^{-1}\sum_\sigma \int_{-\infty}^{\infty} dE\, f(E)\,\mathrm{Im}\{[E - \tfrac{1}{2}\Sigma^{\sigma}(E)]\,G_{00}^{\sigma}(E)\}. \tag{16}$$

The resulting ninth-order equation for our solution from Eq. (13) has, in general, nine roots. Fortunately, in the limit $I/\Delta \geq \frac{1}{2}\sqrt{3}$ for the work discussed in Sec. III, there exist in most cases only two inequivalent solutions for which $\mathrm{Im}G_{00}^{\sigma}(E) \neq 0$ for at least some E. The physical solution is taken to be that solution for which $-\pi^{-1}\int_{-\infty}^{\infty} dE \times \mathrm{Im}G_{00}^{\sigma}(E) = 1$ for each σ, such that the sum for both spin directions equals 2.

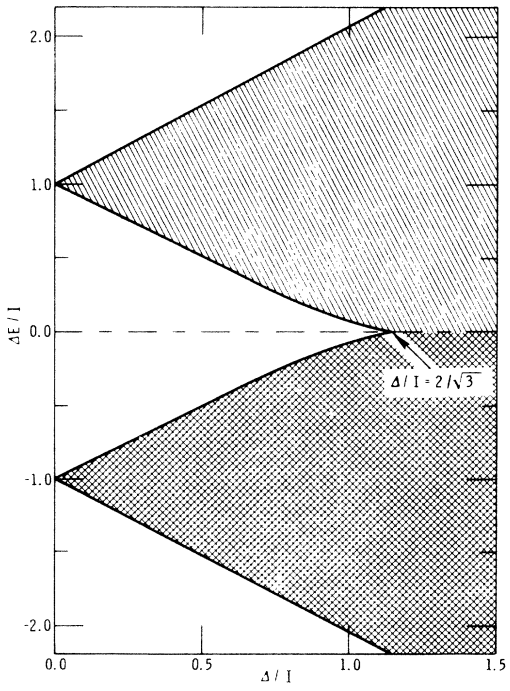

FIG. 1. Energy as a function of the ratio of bandwidth to Coulomb repulsion energy. The upper and lower Hubbard bands merge for $\Delta/I > 2/\sqrt{3}$.

III. RESULTS OF CALCULATIONS

In the following calculations, we have obtained g_σ^+ from Eq. (13) by a computer program (from the Sandia Mathematical Program Library) that solves for the complex roots of a polynomial with real coefficients. Then, using Eqs. (14)–(16), $\rho_\sigma(E)$, n_σ, and E_T can be calculated. Before we discuss these calculations, we wish to orient the reader by showing in Fig. 1 the pseudoparticle spectrum as a function of Δ/I for the half-filled band case ($n = 1$); this figure is similar to Fig. 5 of Ref. 1. The upper and lower Hubbard bands merge for $\Delta/I > 2/\sqrt{3}$. The high-correlation limit discussed in this paper corresponds to the region $\Delta/I < 2/\sqrt{3}$.

A. Ground state

The energy of the paramagnetic state ($m = 0$) is to be compared to the energy of the completely spin-polarized ferromagnetic state ($m = n$). The energy of the $m = 0$ state is calculated using Eqs. (13) and (16). For $m = n = n_\sigma$, $n_{-\sigma} = 0$, and, from

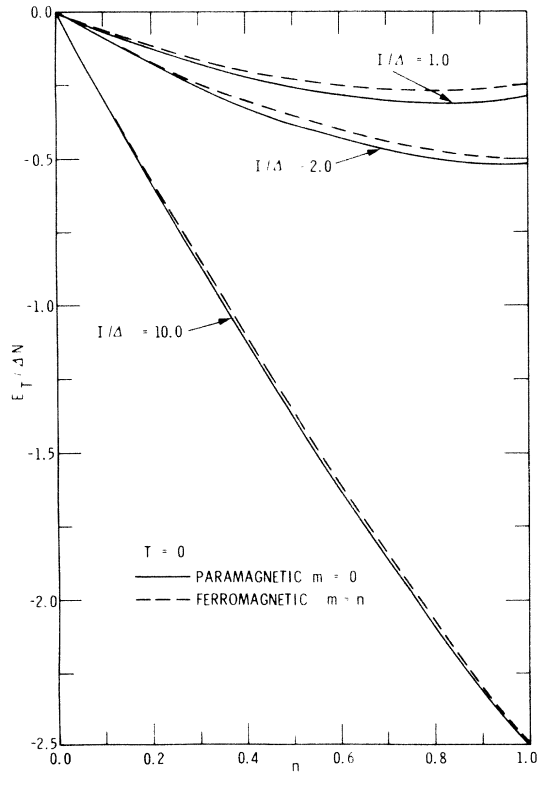

FIG. 2. Electronic energy at $T = 0$ as a function of electron density n. The solid curves are for the paramagnetic energy, while the dashed curves are for the completely spin-polarized ferromagnetic state. Δ is the bandwidth, and N is the number of atoms per unit volume.

Eq. (3), it is clear that $\Sigma^{\sigma}(E) = -\frac{1}{2}I$. Hence $\rho_{\sigma}(E) = \rho^{(0)}(E + \frac{1}{2}I)$, and the energy is then obtained using Eq. (16). It is noteworthy that for $n = 1$, self-consistent solutions exist for all m.[7] This indicates that the $n = 1$ (half-filled band) case is special. As will be pointed out in Sec. III E, for $n = 1$ and in the strong-correlation limit, the susceptibility can be defined only by taking the limit as $n \to 1$. It is our feeling that in this limit the system is also nonferromagnetic, as is the case for $0 \leq n < 1$. We have not investigated possible antiferromagnetic solutions.

In Fig. 2 we illustrate the behavior of E_T vs n, where E_T was calculated using Eq. (16). The difference between the paramagnetic ($m = 0$) and the ferromagnetic ($m = n$) energies decreases as I/Δ increases, with the $m = 0$ solution always having the lower energy, even in the limit of very large I/Δ. The energy difference between the paramagnetic and ferromagnetic states is expected to be that energy required to make the ferromagnetic state the ground state at $T = 0$. This energy difference is shown in Fig. 3. Note that, for large I/Δ, the energy difference between the two states becomes very small, and for $I/\Delta \to \infty$, the energy difference appears to vanish.[14]

Nagaoka[15] obtained a ferromagnetic ground state for very large I/Δ with $n < 1$ (nearly half-filled band) and selected density of states distributions. Even with the circular density of states used here, a ferromagnetic ground state occurs when spin-flip scattering is omitted.[8] We suggest that the absence of a ferromagnetic ground state is due either to (i) excessive dominance of the spin-flip scattering term, which may be moderated by higher-order scattering mechanisms that are omitted in this order decoupling; or to (ii) the choice of the single-particle density of states. We feel that the presence of the ferromagnetic ground state in Nagaoka's work must be reexamined to include spin-flip scattering.

In the low-electron-density limit, Kanamori[16] obtained a ferromagnetic solution. Kanamori used an adaptation of Brueckner's theory for multiple scattering between particles. He found that correlation reduces the intra-atomic interaction I from its bare value. He then constructed a suitable density of states that yielded the Stoner criterion for a ferromagnetic instability, $I_{\text{eff}}\rho^{(0)}(E_f) \geq 1$, where $\rho^{(0)}(E)$ is the suitable single-particle density of states, and I_{eff} is an effective value of I

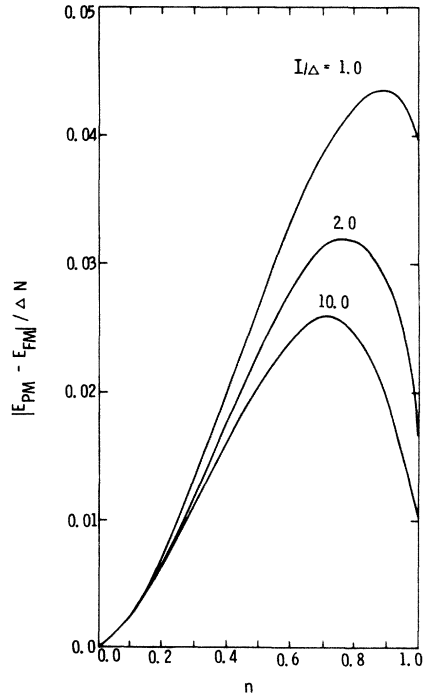

FIG. 3. Difference in energy between the paramagnetic (PM) and ferromagnetic (FM) configurations as a function of electron density n at $T = 0$. The paramagnetic state has the lower energy. Δ is the bandwidth and N is the number of atoms per unit volume.

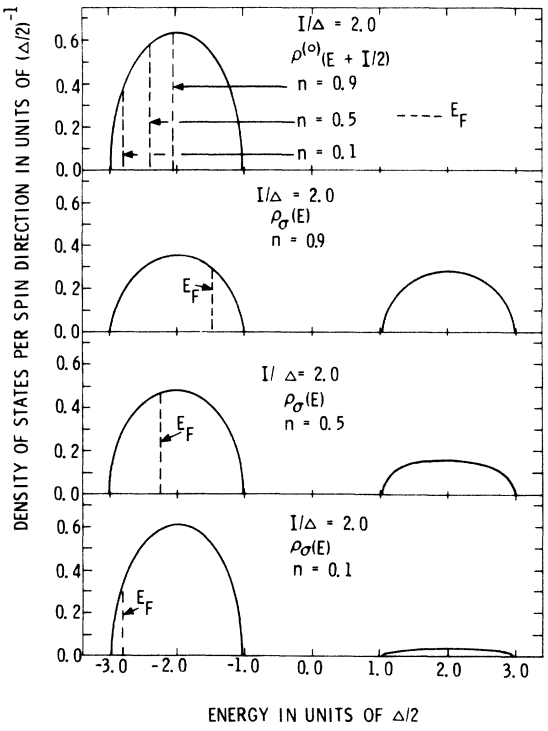

FIG. 4. Density of states per spin direction per atom in units of $(\frac{1}{2}\Delta)^{-1}$ as a function of energy in units of $\frac{1}{2}\Delta$, where Δ is the bandwidth. In the top panel we show the bare density of states $\rho^{(0)}(E)$, and in the bottom three panels we show the pseudoparticle density of states for $n = 0.9$, 0.5, and 0.1, with $I/\Delta = 2.0$.

approximately corrected for multiparticle scattering. The Kanamori theory does not take into account the renormalization of the density of states due to many-body effects, as does the work of this paper, nor does it treat the problem self-consistently. As will become apparent in the work to follow, the pseudoparticle density of states, in particular the density of states at the Fermi level, can differ significantly from the single-particle density of states.

B. Density of states

The pseudoparticle density of states calculated using Eqs. (13) and (14) for $n=0.9$, 0.5, and 0.1 is shown in Fig. 4. Note that the upper bands at energy $\frac{1}{2}I$ contain fewer states for $n<1$. The number of states in the upper σ band is equal to the total possible number of doubly occupied sites per σ spin particle, which decreases from $\frac{1}{2}$ as the occupancy of the band becomes less than half full. The states lost in the upper band appear in the lower band and correspond to the unoccupied sites, of which there are $(1-n)$ per spin band.

The pseudoparticle density of states at the Fermi level $\rho(E_F)$ for the paramagnetic configuration, shown in Fig. 5, differs significantly from that for the single-particle density of states. For example, the single-particle density of states is

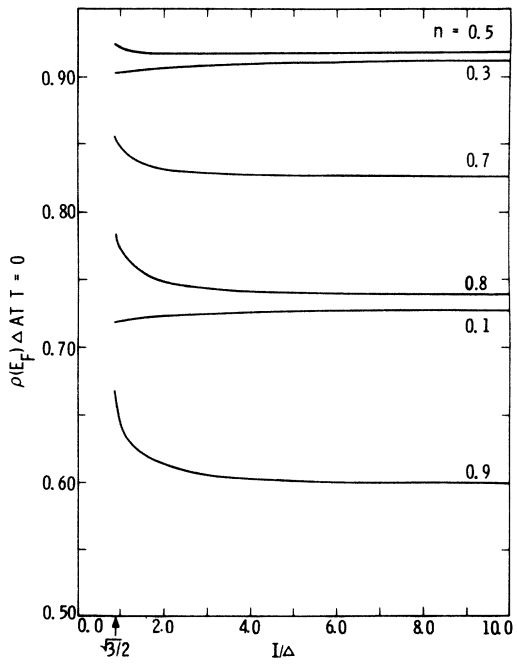

FIG. 5. Pseudoparticle density of states at the Fermi level as a function of the ratio I/Δ for various electron densities n and at $T=0$. $I/\Delta \geq \frac{1}{2}\sqrt{3}$ represents the strong-correlation limit.

symmetrical about $n=1.0$, while the pseudoparticle density of states is not. In addition, $\rho^{(0)}(E_F)$ is at least 20–30% larger than $\rho(E_F)$ for most band occupancies. The reason for the difference between $\rho(E_F)$ and $\rho^{(0)}(E_F)$ is due, of course, to the renormalization of the density of states. One major result of that renormalization in the strong-correlation limit is that the total number of states in the lower Hubbard band (σ plus $-\sigma$ spin bands) is proportional to the occupancy and is approximately equal to $(2-n)$, while the total number of states in the upper Hubbard band is equal to n. For an explanation of this behavior, see Sec. IV.

C. Specific heat

Differentiating Eq. (16) with respect to T gives the result

$$C_V = -\pi^{-1}\sum_\sigma \int_{-\infty}^{\infty} dE \left(\frac{E-E_F}{T}+\frac{\partial E_F}{\partial T}\right)\left|\frac{\partial f(E)}{\partial E}\right| \times \mathrm{Im}\{[E-\tfrac{1}{2}\Sigma^\sigma(E)]\,G_{00}^\sigma(E)\}, \tag{17}$$

where $\partial E_F/\partial T$ can be determined from $\partial n/\partial T=0$ to give

$$\frac{\partial E_F}{\partial T} = -\left(\pi^{-1}\sum_\sigma \int_{-\infty}^{\infty} dE\,(E-E_F)\left|\frac{\partial f(E)}{\partial E}\right| \mathrm{Im}G_{00}^\sigma(E)\right) \times \left(\pi^{-1}T\sum_\sigma \int_{-\infty}^{\infty} dE \left|\frac{\partial f(E)}{\partial E}\right| \mathrm{Im}G_{00}^\sigma(E)\right)^{-1}. \tag{18}$$

Calculations of E_T using Eq. (16) give the result that, at low temperatures, E_T depends on T quadratically, so that we can write $E_T=\frac{1}{2}\gamma T^2$ such that the specific heat at constant volume is $C_V=\gamma T$ for $T\to 0$. From the initial slope of E_T vs T^2, or from Eqs. (17) and (18), we have determined γ as a function of n for various I/Δ. The calculations of γ using Eqs. (17) and (18) give identical results to those using the slope of E_T vs T^2. To illustrate the behavior of γ, we have plotted in Fig. 6 γ vs n for $I/\Delta=2.0$.

The simple theory for the electronic heat coefficient γ in the single-particle picture yields the result that

$$\gamma = \tfrac{2}{3}(\pi k_B)^2\rho^{(0)}(E_F), \tag{19}$$

where $\rho^{(0)}(E_F)$ is the single-particle density of states given by, say, Eq. (7). The results for γ vs n, calculated using Eq. (19), are shown in Fig. 6. In addition, we show the calculation of γ vs n for $I/\Delta=2.0$, where we have replaced the single-particle density of states $\rho^{(0)}(E_F)$ in Eq. (19) by the pseudoparticle density of states $\rho(E_F)$ (Fig. 5). The decrease in γ near $n=1$ is caused

by the decreasing pseudoparticle density of states near the Mott-Hubbard gap.

A comparison of the three curves in Fig. 6 shows quite graphically the differences between a single-particle picture and the interacting electron picture. The electronic energy for noninteracting particles is given by

$$E_T^{(0)} = \int_{-\infty}^{\infty} dE f(E) E \rho^{(0)}(E), \tag{20}$$

and the resulting γ is given by the dot-dash curve in Fig. 6. Replacing $\rho^{(0)}(E)$ by the pseudoparticle density of states $\rho(E)$ defined by Eq. (14) gives the γ shown as the dashed curve in Fig. 6. Finally, using the correct expression for the electronic energy of an interacting system of electrons, Eq. (16), the resulting γ is given by the solid curve in Fig. 6. For a system of interacting electrons, the total energy given by Eq. (16) takes into account the electron self-energy. The difference between the dot-dashed and dashed curves is the self-energy contribution to the density of states at the Fermi level. The difference between the dashed and solid curves is the contribution of the self-energy to the total energy. A comparison of the dashed and solid curves shows that, in calculating thermodynamic properties, in particular the total energy and specific heat, one is *not* at liberty to assume noninteracting single particles, nor simply to replace the single-particle density of states with a pseudoparticle density of states. Thus, correlation introduces an *additional* decrease in γ beyond the value expected from Eq. (19), using the pseudoparticle density of states.

In Fig. 7 we show our results for the specific heat, given by Eqs. (17) and (18), as a function of temperature for various n, and for $I/\Delta = 2.0$. These results are in agreement with the calculations of C_V obtained from E_T by taking finite temperature intervals. The low-temperature peak in C_V shifts toward higher temperatures, and the height of this peak is largest for electron densities of $n \cong 0.5$.

At high temperatures C_V develops a second peak

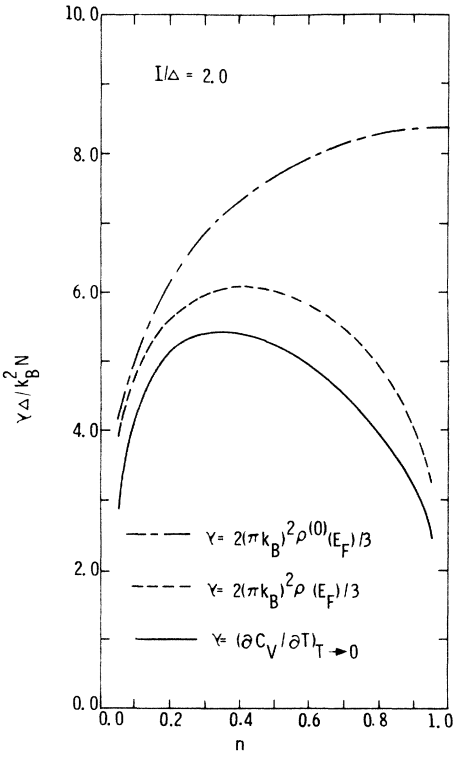

FIG. 6. Electronic specific-heat coefficient γ as a function of electron density n. The solid curve was calculated using the electronic energy defined by Eq. (16) and C_V defined by Eq. (17), while the dot-dashed and dashed curves were calculated using the single-particle formula with the single-particle and pseudoparticle densities of states, respectively. N is the number of atoms per unit volume.

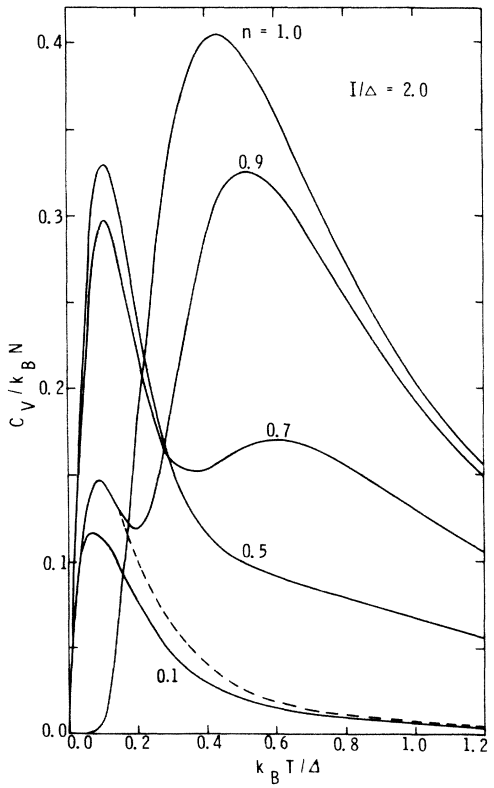

FIG. 7. Electronic specific heat C_V as a function of temperature for various electron densities n with $I/\Delta = 2.0$. These results were obtained using Eq. (17). A calculation of C_V for $n = 0.9$ in which the contribution of the upper Hubbard band is ignored is shown by the dashed curve. N is the number of atoms per unit volume.

for $n<1$ which shifts to higher temperatures as the electron density is decreased. The height of this high-temperature peak decreases as n decreases, and is barely noticeable for $n=0.5$. This peak appears to be associated with excitations across the Mott-Hubbard gap, and not with magnetic ordering. In support of this assertion, the contribution to C_V from the states in the upper Hubbard band were determined by omitting these states in the integral of Eq. (17). As a result, the high-temperature peak disappeared, as shown by the dashed curve of Fig. 7 for $n=0.9$. This behavior indicates that the high-temperature peak in C_V is due entirely to these excitations. In addition, this result, along with the $n=1$ curve, suggests that the low-temperature peak is caused by excitations into states immediately above E_F in the lower band. It appears, therefore, that the structure in the specific heat is due entirely to structure in the density of states. As will be seen in Sec. III D, no corresponding peaks occur in the magnetic properties.

D. Magnetic susceptibility

The reduced paramagnetic susceptibility for a uniform magnetic field is given by

$$\chi_r(T)\equiv\left(\frac{\partial m}{\partial H}\right)_{H\to 0}=2\left(\frac{\partial n_+}{\partial H}\right)_{H\to 0}, \tag{21}$$

where the susceptibility $\chi(T)=\mu_B^2 N\chi_r(T)$, with N the number of atoms per unit volume. Using Eq. (15), and following Fukuyama and Ehrenreich,[6] Eq. (21) becomes

$$\chi_r(T)=2\chi_0(T)(1+K)^{-1}, \tag{22}$$

where

$$\chi_0(T)=-\pi^{-1}\int_{-\infty}^{\infty}dE\left|\frac{\partial f(E)}{\partial E}\right|\mathrm{Im}G_{00}^{+}(E), \tag{23}$$

and

$$K\equiv\frac{\partial n_+}{\partial n_-}=-\pi^{-1}\int_{-\infty}^{\infty}dE f(E)\,\mathrm{Im}\,\frac{\partial G_{00}^{+}(E)}{\partial n_-}. \tag{24}$$

$\chi_0(T)$ represents the unenhanced susceptibility and, in the limit $T\to 0$, $\chi_0(0)=\rho(E_F)$, in agreement with Fukuyama and Ehrenreich.[6] Here $(1+K)$ is the enhancement factor, and a ferromagnetic instability will occur for finite temperature when, and if, $K=-1$.

From the four equations in $\pm\sigma$ and $\pm E$ represented by Eq. (11), $\partial G_{00}^{+}(E)/\partial n_-\equiv\partial g_+^+/\partial n_-$ can be calculated. Replacing n_+ by $(n-n_-)$ and treating n_- as the independent variable, we obtain four equations for the four unknowns $\partial g_+^+/\partial n_-$, $\partial g_-^+/\partial n_-$, $\partial g_+^-/\partial n_-$, and $\partial g_-^-/\partial n_-$. After completing the differentiation, we set $m=0$ such that g_-^+ and g_+^+ and $g_+^-=g_-^-$. The set of simultaneous equations is illustrated in matrix form

$$R\left(\frac{\partial g}{\partial n_-}\right)=S, \tag{25}$$

and is shown in some detail in Appendix B.

The temperature dependence of $\chi(T)$, calculated from Eqs. (22)–(25), is shown in Fig. 8 for various occupancies and $I/\Delta=2.0$. K is nearly temperature independent for all n and for temperatures up to $k_BT/\Delta\cong 0.1$, and hence the temperature dependence is due primarily to $\chi_0(T)$. For $k_BT/\Delta\gtrsim 0.1$, K takes on some temperature dependence. Contributions to the temperature dependence in the regime $I/\Delta\gtrsim 2.0$ from single-particle excitations across the gap in the density of states are insignificant at low temperatures.

At lower temperatures, $\chi(T)$ is temperature independent, and at the higher temperature, $\chi(T)$ takes on a Curie-like behavior. At high temperatures, $I\chi(T)/\mu_B^2N$ is linear with respect to I/k_BT, and the slopes of the various curves approach n.

Our results for $\chi(T)$ are in semiquantitative agreement at the high temperatures with those of Beni, Pincus, and Hone[17] for a simple cubic lattice. Their high-temperature slopes are n for low electron densities, but are somewhat less than n for the band being nearly half-filled. At the lower temperatures our results, Fig. 8, show

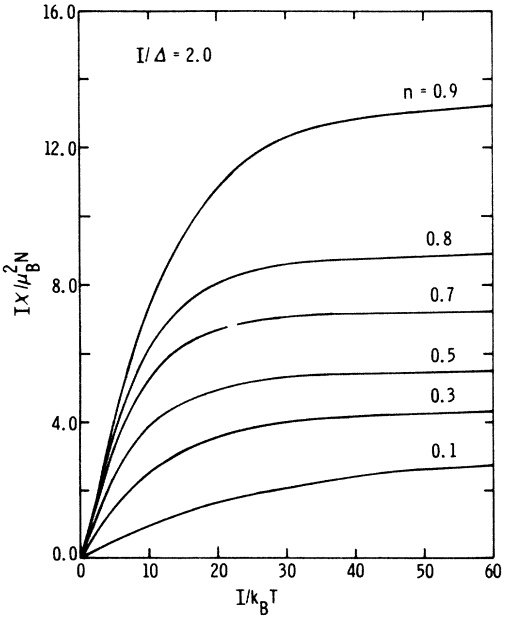

FIG. 8. Magnetic susceptibility as a function of the inverse temperature at various electron densities n. Here we show the calculation for $I/\Delta=2.0$ using Eq. (22). N is the number of atoms per unit volume.

a definite Pauli-like behavior for all electron densities, whereas Beni *et al.*[17] obtain a maximum in the susceptibility, which they interpret as indicative of a transition to an antiferromagnetic state for the half-filled and nearly half-filled bands, while a concave upward behavior is interpreted as indicative of a transition to a ferromagnetic state at the lower electron densities. We obtain neither a maximum nor the concave upward behavior, and suspect that the differences are caused by poor convergence of their series expansion in this temperature region.

The temperature dependence of $\chi(T)$ may be understood at high temperature by investigation of the spin-correlation function and at low temperature by investigation of the dependence of $\rho(E_F)$ on correlation energy.

1. *High-temperature susceptibility*

At high temperatures, the reduced paramagnetic susceptibility for localized spins must be proportional to the single-site spin correlation function

$$\chi(T)_{\rm loc} = g^2 L_0(T)/3k_B T\,, \tag{26}$$

where g is the usual g factor and $L_0(T)$ is given by[9]

$$L_0(T) = \frac{3}{N}\sum_j \langle (S_j^z)^2\rangle = \frac{3}{2N}\sum_j \langle n_{j\uparrow}(1-n_{j\downarrow})\rangle\,, \tag{27}$$

in the paramagnetic regime. From Hubbard's[1] Eq. (49), replacing the resonance-broadening interactors by total interactor $\Omega_\sigma(E)$, and from his Eqs. (50) and (59), along with our Eq. (3), we can calculate the Green's function $\langle\langle n_{i-\sigma}C_{i\sigma};\ C_{i\sigma}^{\dagger}\rangle\rangle$. From this Green's function the correlation function in Eq. (27) can be evaluated for arbitrary occupancy as

$$L_0(T) = \frac{3}{4}\int_{-\infty}^{\infty} dE\, f(E)\left(-\frac{1}{\pi}\right)\mathrm{Im}\left(\frac{\frac{1}{2}I - \Sigma^{\sigma}(E)}{\frac{1}{2}I}\, G_{00}^{\sigma}(E)\right) \tag{28}$$

in agreement with Eq. (4.16) of Shiba and Pincus,[9] wherein $F^{\sigma}(E) = E - \Sigma^{\sigma}(E)$ (see also Ref. 4).

At this temperature, and in the strong correlation regime, $\langle n_{j\uparrow}n_{j\downarrow}\rangle \to 0$, with the result that $L_0(T) \to \frac{3}{4}n$. Therefore,

$$\chi_{\rm loc} = \tfrac{3}{4}\, ng^2/3k_B T = n(k_B T)^{-1}\,, \tag{29}$$

as expected from the well-known susceptibility expression for a localized moment, $\chi_{\rm loc} = ng^2 S(S+1)/3k_B T$ for $S = \frac{1}{2}$.

At extreme temperatures, the spins become uncorrelated and $\langle n_{j\uparrow}n_{j\downarrow}\rangle \to \langle n_{j\uparrow}\rangle\langle n_{j\downarrow}\rangle$ yielding the result $L_0(T) \to \frac{3}{4}n(1-\frac{1}{2}n)$ and

$$\chi_{\rm loc} = n(1-\tfrac{1}{2}n)g^2 S(S+1)/3k_B T = n(1-\tfrac{1}{2}n)(k_B T)^{-1}\,. \tag{30}$$

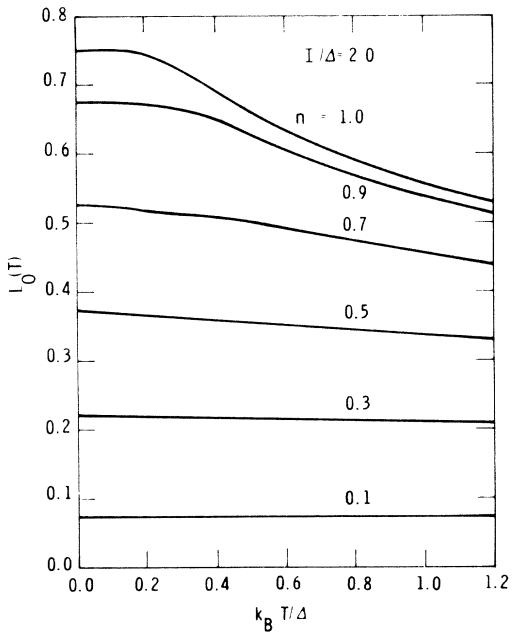

FIG. 9. Single-site spin-correlation function $L_0(T)$ as a function of temperature for various electron densities n and $I/\Delta = 2.0$. $L_0(T)$ was calculated using Eq. (28). At $T = 0$, $L_0(T)$ is equal to the correlated value of $\frac{3}{4}n$. At high temperatures, $L_0(T)$ approaches the uncorrelated value of $\frac{3}{4}n(1-\frac{1}{2}n)$.

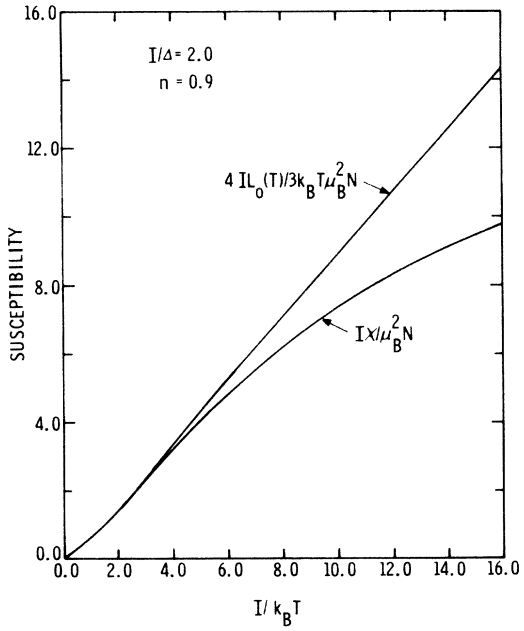

FIG. 10. Comparison of $I\chi/\mu_B^2 N$ and $4IL_0(T)/3k_B T\mu_B^2 N$ as a function of inverse temperature. Here $\chi(T)$ was calculated using Eq. (22), and $L_0(T)$ was calculated using Eq. (28) for $n = 0.9$ and $I/\Delta = 2.0$.

The temperature dependence of $L_0(T)$ for various occupancies is shown in Fig. 9 for $I/\Delta = 2.0$. At intermediate temperature, $\chi(T)$ equals approximately the correlated value [Eq. (29)]; at high temperature, $\chi(T)$ approaches the uncorrelated value [Eq. (30)]. Figure 10 compares the susceptibility calculated from Eq. (26) with the susceptibility for $n = 0.9$ obtained from Fig. 8. The agreement between $\chi(T)$ and Eq. (26) in the highest temperature region is good, indicating that the susceptibility is due mostly to uncorrelated localized spins. As temperature decreases, the deviation between the two curves is small, indicating that some correlation has developed between spins at intermediate temperature. However, large deviations occur for $I/k_BT > 6.0$, indicating that higher-order correlation functions now dominate the susceptibility, and that Eq. (26) is not a good approximation.

2. *Low-temperature susceptibility*

These higher-order correlations cause $\chi(T)$ to asymptotically approach a temperature-independent value

$$\chi(0) = 2\rho(E_F)/[1 + K(0)] \,. \tag{31}$$

The enhancement factor $K = \partial n_+/\partial n_-$ is given in Fig. 11 as a function of I/Δ; the susceptibility [Eq. (31)] is shown in Fig. 12 for various occupancies. K and $\chi(0)$ are nearly independent of I/Δ for $I/\Delta \simeq 2$–3, but near the critical value, $\frac{1}{2}\sqrt{3}$, some dependence on I/Δ develops. The asymptotic values of $\chi(T)$ in Fig. 8 are just the values of $\chi(0)$ in Fig. 12 at $I/\Delta = 2.0$.

Thus we see that, although a temperature-independent Pauli-like susceptibility exists at the lowest temperatures, the susceptibility is enhanced over that expected from the free-electron value $2\rho(E_F)$. This enhancement factor reflects the nearness of the band to half-filled, at which point the susceptibility becomes Curie-like. For the half-filled band ($n = 1$) at $T = 0$, $K = -1$ and $\rho(E_F) = 0$ such that $\chi(0)$, Eq. (31), is undefined and can only be defined in the limit $n \to 1$; in this limit $\chi(0)$ appears to have Curie-like behavior. At low density, where a large number of unoccupied states occur above E_F, the enhancement is least, and the susceptibility most closely approaches the free-electron value.

In the Hartree-Fock theory, the reduced exchange-enhanced susceptibility at $T = 0$ is given by

$$\chi_{\mathrm{HF}} = \frac{2\rho^{(0)}(E_F)}{1 - I\rho^{(0)}(E_F)} \,. \tag{32}$$

It is tempting to replace $\rho^{(0)}(E_F)$ by the pseudoparticle density of states at the Fermi level $\rho(E_F)$, and to replace I by an effective I_{eff}. Comparing Eqs. (31) and (32), $I_{\mathrm{eff}}\rho(E_F) = -K$, at $T = 0$. $\rho(E_F) \sim \Delta^{-1}$, and in Kanamori's[16] theory $I_{\mathrm{eff}} \sim \Delta$ in the strong-correlation limit. Thus, in the strong-

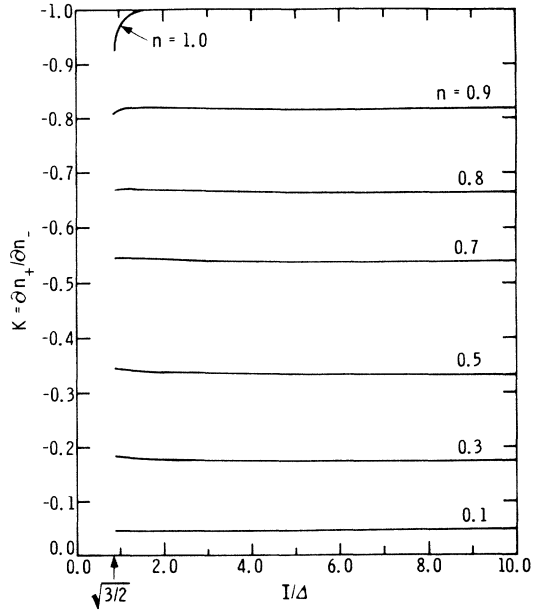

FIG. 11. Enhancement factor K at $T = 0$ as a function of the ratio I/Δ at various electron densities n. For $I/\Delta \gtrsim 2.0$ and $n = 1.0$, $K = -1$. $I/\Delta \geq \frac{1}{2}\sqrt{3}$ represents the strong-correlation limit.

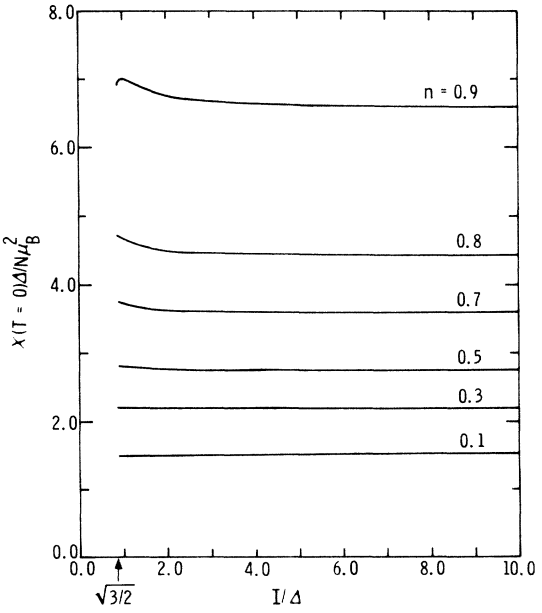

FIG. 12. Magnetic susceptibility at $T = 0$ as a function of the ratio I/Δ for various electron densities n. $I/\Delta \geq \frac{1}{2}\sqrt{3}$ represents the strong-correlation limit.

correlation limit $I_{\text{eff}}\rho(E_F)$ = constant, independent of I/Δ. This result agrees with our findings that K is nearly independent of I/Δ in the strong-correlation limit (see Fig. 11).

IV. SUMMARY AND CONCLUSIONS

In this paper we have obtained the solution to the Hubbard model Hamiltonian that includes all three scattering terms of Hubbard, spin-disorder (analogous to potential scattering in an alloy) and the two resonance-broadening terms, scattering of a σ spin electron into a $-\sigma$ spin hole, and spin-flip scattering. For a semicircular, single-particle density of states, the solution is accomplished using a locator technique,[10,11] the result of which is a ninth-order equation in the local Green's function, the imaginary part of which is the average pseudoparticle density of states. Our solution contains no approximations beyond those contained in the locator technique, and in the selection for the functional form of the bare density of states. No high-temperature expansion, and no expansion in Δ/I, has been assumed. In the locator technique, it is assumed that the scattering rate for an average atom at the origin in a lattice of atoms is equal to the configurational average of the scattering by the various component atoms replacing the average atom at the origin. This locator formulation is equivalent to Hubbard's truncation of the Green's-function equation of motion beyond two-particle scattering terms. The solution, Eq. (13), is valid for all band occupancies and strengths of the Coulomb repulsion. However, we restrict our discussions here to the strong-correlation limit and to paramagnetic and completely ferromagnetic regimes only.

From the work in this paper and our previous work,[7,8] we find that the CPA, which takes into account only spin-disorder scattering, and ignores the resonance-broadening terms, leads to qualitatively different results from those obtained when all three of Hubbard's scattering terms are included. We conclude that the CPA biases the solution in favor of the ferromagnetic state. There seems to be no compelling reason why a single-site intra-atomic correlation should lead to a ferromagnetic ground state. In fact, it is argued that, for a half-filled band, the antiferromagnetic state[18] is the lower energy configuration. The absence of a ferromagnetic ground state in our work agrees with the doubt about the possibility of ferromagnetism without band degeneracy.[18] Therefore, we conclude that any solution to the Hubbard model must not ignore spin-flip scattering. For the fully polarized ferromagnetic case, the energy difference between the ferromagnetic and the paramagnetic states is at most 0.044Δ for I/Δ as small as 1.0, and becomes smaller as I/Δ increases. By direct calculation, this energy difference corresponds to the magnetic or molecular-field energy required to produce the $m = n$ ferromagnetic ground state. Thus, a weak interatomic ferromagnetic exchange could provide this difference. Our results, therefore, lead to an energy separation between the ferromagnetic and paramagnetic states that is of the order of magnitude commonly expected from experimentally observed Curie temperatures. This result is to be contrasted with the Stoner-Hartree-Fock results in which this energy difference can be as large as the correlation energy.[18]

The specific heat and magnetic susceptibility differ from the one-dimensional calculations of Shiba and Pincus[9] and Shiba,[19] probably because our single-particle density of states vanishes at the band edge, while for the one-dimensional case, there is a singularity at the band edge. Our high-temperature susceptibility calculations obey a Curie law and are in semiquantitative agreement with Beni *et al.*[17] However, at lower temperatures, our susceptibility displays Pauli behavior, whereas their lower-temperature susceptibility for the simple cubic density of states displays tendencies toward an antiferromagnetic state for half-filled and nearly-half-filled bands, and toward a ferromagnetic state for the low electron density. These differences may arise from poor convergence in their high-temperature expansion.

We find that the total number of states in the lower Hubbard band for a less than half-filled band is $2 - n$, while the total number in the upper band is n. This result is in qualitative agreement with the predictions of Harris and Lange[20]; see Eqs. (5.20a) and (5.20b) of Ref. 20, where the correlation function $\langle C_{i-\sigma}{}^{\dagger} C_{j-\sigma}\rangle$ is negative for a less than half-filled band. When hopping is *not* allowed, the total number of states in the lower and upper bands is $2 - n$ and n, respectively. When hopping is allowed, there are effectively fewer occupied sites (less chance for double occupancy) because the electron clears a space for itself due to the repulsion, and the total number of states in the lower and upper bands becomes greater than $2 - n$, and less than n, respectively. In our work for $I/\Delta \gtrsim 1.25$, the number of states is given by $2 - n$ and n to within the accuracy of the calculations. Evidently, in the regime $I/\Delta > 1.25$, the correlation function $\langle C_{i-\sigma}{}^{\dagger} C_{j-\sigma}\rangle$ is small. Investigation of the $I/\Delta < 1.25$ regime is in progress.

Finally, we note that simply replacing the single-particle density of states by the pseudoparticle density of states in the electronic specific heat for a system of strongly interacting particles

omits a self-energy contribution that reduces the specific heat approximately 10–20% more for $I/\Delta = 2.0$.

APPENDIX A

Equation (13) represents two coupled equations for g^{+}_{σ} and $g^{-}_{-\sigma}$, where $g^{-}_{\sigma} \equiv G^{\sigma}_{00}(E)$ and $g^{-}_{-\sigma} \equiv G^{-\sigma}_{00}(-E)$. The coupled equations for g^{+}_{+} and g^{-}_{-} become

$$\sum_{i=0}^{3} a_i (g^{+}_{+})^{3-i} + \sum_{i=0}^{2} b_i (g^{+}_{+})^{2-i} g^{-}_{-} = 0, \tag{A1}$$

$$\sum_{i=0}^{3} c_i (g^{-}_{-})^{3-i} + \sum_{i=0}^{2} d_i (g^{-}_{-})^{2-i} g^{+}_{+} = 0, \tag{A2}$$

where

$$\begin{aligned} &a_0 = c_0 = -\tfrac{1}{8}, \quad b_0 = d_0 = +\tfrac{1}{16}, \\ &b_2 = d_2 = +\tfrac{1}{4}, \quad a_2 = c_2 = (\tfrac{1}{2}I)^2 - E^2 - \tfrac{1}{2}, \\ &a_1 = \tfrac{3}{4}E + \tfrac{1}{4}\Gamma_{-}, \quad a_3 = E - \Gamma_{-}, \\ &b_1 = -\tfrac{1}{4}(E + \Gamma_{-}), \quad d_1 = -\tfrac{1}{4}(-E + \Gamma_{+}). \\ &c_1 = -\tfrac{3}{4}E + \tfrac{1}{4}\Gamma_{+}, \quad c_3 = -E - \Gamma_{+}. \end{aligned} \tag{A3}$$

Solving Eq. (A1) for g^{-}_{-},

$$g^{-}_{-} = -\sum_{i=0}^{3} a_i (g^{+}_{+})^{3-i} \Big/ \sum_{i=0}^{2} b_i (g^{+}_{+})^{2-i}, \tag{A4}$$

and substituting this result into Eq. (A2), the resulting equation is ninth order for g^{+}_{+} such that

$$\sum_{i=0}^{9} \xi_i (g^{+}_{+})^{9-i} = 0. \tag{A5}$$

Here the coefficients ξ_i are given by

$$\begin{aligned} \xi_0 &= A_0 C_0, \\ \xi_1 &= A_0 C_1 + A_1 C_0 + B_0 D_0, \\ \xi_2 &= A_0 C_2 + A_1 C_1 + A_2 C_0 + B_0 D_1 + B_1 D_0, \\ \xi_3 &= A_0 C_3 + A_1 C_2 + A_2 C_1 + A_3 C_0 + B_0 D_2 + B_1 D_1 + B_2 D_0, \\ \xi_4 &= A_1 C_3 + A_2 C_2 + A_3 C_1 + A_4 C_0 \\ &\quad + B_0 D_3 + B_1 D_2 + B_2 D_1 + B_3 D_0, \\ \xi_5 &= A_2 C_3 + A_3 C_2 + A_4 C_1 + A_5 C_0 \\ &\quad + B_0 D_4 + B_1 D_3 + B_2 D_2 + B_3 D_1 + B_4 D_0, \\ \xi_6 &= A_3 C_3 + A_4 C_2 + A_5 C_1 + A_6 C_0 \\ &\quad + B_1 D_4 + B_2 D_3 + B_3 D_2 + B_4 D_1, \\ \xi_7 &= A_4 C_3 + A_5 C_2 + A_6 C_1 + B_2 D_4 + B_3 D_3 + B_4 D_2, \\ \xi_8 &= A_5 C_3 + A_6 C_2 + B_3 D_4 + B_4 D_3, \quad \xi_9 = A_6 C_3 + B_4 D_4, \end{aligned} \tag{A6}$$

where

$$\begin{aligned} &A_0 = a_0^2, \quad A_1 = 2a_0 a_1, \quad A_2 = a_1^2 + 2a_0 a_2, \\ &A_3 = 2(a_0 a_3 + a_1 a_2), \quad A_4 = a_2^2 + 2a_1 a_3, \\ &A_5 = 2a_2 a_3, \quad A_6 = a_3^2; \\ &B_0 = b_0^2, \quad B_1 = 2b_0 b_1, \quad B_2 = b_1^2 + 2b_0 b_2, \\ &B_3 = 2b_1 b_2, \quad B_4 = b_2^2; \\ &C_0 = d_0 b_0 - c_0 a_0, \quad C_1 = d_0 b_1 + c_1 b_0 - a_1 c_0, \\ &C_2 = d_0 b_2 + c_1 b_1 - c_0 a_2, \quad C_3 = c_1 b_2 - c_0 a_3; \\ &D_0 = -d_1 a_0, \quad D_1 = d_2 b_0 - d_1 a_1 - c_2 a_0, \\ &D_2 = d_2 b_1 + c_3 b_0 - d_1 a_2 - c_2 a_1, \\ &D_3 = (d_2 b_2 + c_3 b_1 - d_1 a_3 - c_2 a_2), \quad D_4 = c_3 b_2 - c_2 a_3. \end{aligned} \tag{A7}$$

To find g^{-}_{-}, the solution for g^{+}_{+} is then substituted into Eq. (A4).

APPENDIX B

Equation (11) represents four coupled equations for g^{+}_{+}, g^{+}_{-}, g^{-}_{+}, and g^{-}_{-} where $g^{\pm}_{\pm\sigma} \equiv G^{\pm\sigma}_{00}(\pm E)$. Replacing n_{+} by $n - n_{-}$ in Eq. (11), and treating n_{-} as the independent variable, we differentiate these four equations with respect to n_{-} and obtain

$$\begin{pmatrix} R_1 & -R_2 & 0 & R_2 \\ -R_2 & R_1 & R_2 & 0 \\ 0 & R_4 & R_3 & -R_4 \\ R_4 & 0 & -R_4 & R_3 \end{pmatrix} \begin{pmatrix} \partial g^{+}_{+}/\partial n_{-} \\ \partial g^{+}_{-}/\partial n_{-} \\ \partial g^{-}_{+}/\partial n_{-} \\ \partial g^{-}_{-}/\partial n_{-} \end{pmatrix} = \begin{pmatrix} S_1 \\ -S_1 \\ S_2 \\ -S_2 \end{pmatrix} \tag{B1}$$

after setting $g^{+}_{-} = g^{+}_{+}$ and $g^{-}_{+} = g^{-}_{-}$ for $m = 0$, the paramagnetic regime. Here

$$\begin{aligned} R_1 &= -\tfrac{5}{16}(g^{+}_{+})^2 + (\tfrac{5}{4}E + \tfrac{1}{4}\Gamma_{-})g^{+}_{+} + (\tfrac{1}{2}I)^2 - E^2 - \tfrac{1}{4} \\ &\quad + \tfrac{1}{8} g^{+}_{+} g^{-}_{-} - \tfrac{1}{4}(E + \Gamma_{-}) g^{-}_{-}, \\ R_2 &= \tfrac{1}{16}(g^{+}_{+})^2 - \tfrac{1}{4}(E + \Gamma_{-}) g^{+}_{+} + \tfrac{1}{4}, \\ R_3 &= -\tfrac{5}{16}(g^{-}_{-})^2 + (-\tfrac{5}{4}E + \tfrac{1}{4}\Gamma_{-}) g^{-}_{-} + (\tfrac{1}{2}I)^2 - E^2 - \tfrac{1}{4} \\ &\quad + \tfrac{1}{8} g^{-}_{-} g^{+}_{+} - \tfrac{1}{4}(-E + \Gamma_{-}) g^{+}_{+}, \\ R_4 &= \tfrac{1}{16}(g^{-}_{-})^2 - \tfrac{1}{4}(-E + \Gamma_{-}) g^{-}_{-} + \tfrac{1}{4}, \\ S_1 &= I[\tfrac{1}{4}(g^{+}_{+})^2 - \tfrac{1}{4} g^{+}_{+} g^{-}_{-} - 1], \\ S_2 &= I[\tfrac{1}{4}(g^{-}_{-})^2 - \tfrac{1}{4} g^{+}_{+} g^{-}_{-} - 1]. \end{aligned} \tag{B2}$$

Equation (B1) can be solved for $\partial g^{+}_{+}/\partial n_{-}$ using standard techniques.

*Work at Sandia Laboratories supported by the U. S. AEC.

[1]J. Hubbard, Proc. R. Soc. A 281, 401 (1964).
[2]D. M. Esterling and H. C. Dubin, Phys. Rev. B 6, 4276 (1972).
[3]P. Soven, Phys. Rev. 156, 809 (1967); 178, 1136 (1969).
[4]B. Velický, S. Kirkpatrick, and H. Ehrenreich, Phys. Rev. 175, 747 (1968).
[5]K. Levin and K. H. Bennemann, Phys. Rev. B 5, 3770 (1972).
[6]H. Fukuyama and H. Ehrenreich, Phys. Rev. B 7, 3266 (1973).
[7]H. S. Jarrett, in *Proceedings of the Eighteenth Annual Conference on Magnetism and Magnetic Materials, No. 10*, edited by C. D. Graham and J. J. Rhyne (AIP, New York, 1973), pp. 521–525.
[8]L. C. Bartel and H. S. Jarrett, in Proceedings of the Nineteenth Annual Conference on Magnetism and Magnetic Materials (unpublished).
[9]H. Shiba and P. A. Pincus, Phys. Rev. B 5, 1966 (1972).
[10]H. Shiba, Prog. Theor. Phys. 46, 77 (1971).
[11]J. A. Blackman, D. M. Esterling, and N. F. Berk, Phys. Rev. B 4, 2412 (1971).
[12]R. A. Bari and T. A. Kaplan, Phys. Lett. A 33, 400 (1970).
[13]B. Kjöllerström, D. J. Scalapino, and J. R. Schrieffer, Phys. Rev. 148, 665 (1966).
[14]R. A. Tahir-Kheli and H. S. Jarrett, Phys. Lett. A 27, 485 (1968).
[15]Y. Nagaoka, Phys. Rev. 147, 392 (1966).
[16]J. Kanamori, Prog. Theor. Phys. 30, 275 (1963).
[17]G. Beni, P. Pincus, and D. Hone, Phys. Rev. B 8, 3389 (1973).
[18]C. Herring, *Magnetism*, edited by G. T. Rado and H. Suhl (Academic, New York, 1966), Vol. IV.
[19]H. Shiba, Phys. Rev. B 6, 930 (1972).
[20]A. B. Harris and R. V. Lange, Phys. Rev. 157, 295 (1967).